Cancer Nano (2013) 4:73–79
DOI 10.1007/s12645-013-0038-3

ORIGINAL PAPER

Fungus-mediated synthesis of silver nanoparticles and evaluation of antitumor activity

S. M. El-Sonbaty

Received: 15 March 2013 / Accepted: 6 May 2013 / Published online: 24 May 2013

Abstract Silver nanoparticles (AgNPs) were biologically synthesized using aqueous extract of *Agaricus bisporus* fungi. Physicochemical analysis of silver nanoparticles revealed that they are of spherical shape ranged size of 8–20 nm, and their zeta potential equal −7.23 mV. Silver nanoparticles showed a dose-dependent cytotoxic effect on MCF-7 breast cancer cells with LD_{50} (50 μg/ml). Mice bearing Ehrlich solid tumor treated with AgNPs and exposed to gamma radiation significantly ameliorated superoxide dismutase and catalase activity and reduced glutathione with an increase in malondialdehyde and nitric oxide levels compared to tumor group. Gamma radiation with AgNPs induced apoptotic cell count in Ehrlich solid tumor cells from 68.3 (treated with AgNPs) to 98.1 % (treated with AgNPs with gamma radiation) via a mechanism involved caspase-3. Histological sections of tumor tissue of mice treated with AgNPs showed antiangiogenesis effect of AgNPs. The overall result indicates that AgNPs synergize with gamma radiation, promising a potential combined therapy of cancer.

Keywords Silver nanoparticles · Ehrlich tumor · Apoptosis · Cell cycle · Caspase

1 Introduction

Nanotechnology is the most promising field for generating new applications in medicine. A green chemistry of nanoparticles synthesis via biological methods using either microorganisms or plant extracts have offered a reliable and ecofriendly alternative to chemical and physical methods to improve and/or protect our global environment. Even though the chemical methods involve a very simple procedure, they employ chemical reducing agents, such as citrate, borohydride, or other organic compounds, which are toxic to living organisms and hence render them unsuitable for medical use, whereas ecofriendly biologic synthesis involves formation of AgNPs by means of enzymatic reduction with better control over the shape and size of the nanoparticles. Biological methods, apart from being cost-effective, also provide protein-capped nanoparticles, which are thus very stable, have good dispersity, and do not flocculate (Law et al. 2008).

Only few nanoproducts are currently in use for medical purposes. A most prominent nanoproduct is nanosilver. Silver nanoparticles have (AgNPs) been shown various therapeutic effects such as antimicrobial, antifungal, antioxidant, and antiinflammatory effects (Tian et al. 2007). Silver NPs have been shown to induce the apoptotic pathway in vitro through free oxygen radical generation also showed antitumor, antiproliferative, and antiangiogenic effect in vitro (Rani et al. 2009; Park et al. 2010; Kalishwaralal et al. 2009).

AgNPs have gained increasing interest in the field of nanomedicine due to their unique properties and obvious therapeutic potential in treating a variety of diseases, including retinal neovascularization and acquired immunodeficiency syndrome due to human immunodeficiency virus. AgNPs are also known for their antimicrobial potential against several other viruses, including hepatitis B, respiratory syncytial virus, herpes simplex virus type, and monkey pox virus. AgNPs and ions have been shown to possess intrinsic cytotoxic activity (Sriram et al. 2010).

Cancer is the most important cause of mortality in the world. Cytotoxic agents used for its treatment are expensive and known to induce several side effects such as anemia and most importantly the generation of cellular resistance. For this, it is important to find alternative therapies or drugs to overcome these drawbacks (Franco-Molina et al. 2010). Although there is a wide range of cytotoxic agents used in the treatment of cancer, such as doxorubicin, cisplatin, and bleomycin, they have shown drawbacks in their use and are not as efficient as

S. M. El-Sonbaty (✉)
Biochemistry, National Center of Radiation Research and Technology, Cairo, Egypt
e-mail: sawsansonbaty@yahoo.com

expected. Therefore, it is of great interest to find novel therapeutic agents against cancer (Franco-Molina et al. 2010).

The aim of our study to determine the antitumor potential effect of biologically synthesized AgNPs in vitro on MCF-7 cell line and in vivo on Ehrlich ascites carcinoma solid tumor.

2 Materials and methods

Biosynthesis and purification of silver nanoparticles Sixty-eight grams of finely cut mushroom *Agaricus bisporus* was boiled in deionized distilled water and filtered. The filtrate was cooled to room temperature and used as reducing agent and stabilizer. Fifty milligrams of $AgNO_3$ were dissolved in 100 ml of the filtrate previously prepared from mushroom. The resulting aqueous solution was filtered through a 0.22 μm Millipore filter before use (Philip 2009).

Characterization of silver nanoparticles Accurate determination of the size and concentration of nanoparticles is essential for the biomedical application of nanoparticles.

The zeta potential measurement Measurements were carried out using a the particle size/zeta potential analyzer, Nicomp 380 ZLS Submicron.

UV–Vis absorbance spectroscopy analysis The bioreduction (of $AgNO_3$) was measured by UV–Vis spectroscopy. The samples used for analysis were diluted with 2 mL deionized water and subsequently measured by the UV–Vis spectrum at regular different time intervals (Rajesh et al. 2010). The UV–Vis spectrometric readings were recorded at a scanning speed of 200 to 800 nm.

TEM analysis of silver nanoparticles Silver nanoparticles of *A. bisporus* was sampled by transmission electron microscopy (TEM) analysis. TEM samples were prepared by placing a drop of the suspension of silver nanoparticles solution on carbon-coated copper grids and allowing water to evaporate. The shape and size of nanoparticles were determined from TEM micrographs The software (Advanced Microscopy Techniques, Danvers, MA) for the digital TEM camera was calibrated for size measurements of the nanoparticles. TEM measurements were performed on a JEOL model 1200EX, (Gurunathan et al. 2009). Zeta potential of AgNPs was measured using TEM.

Cytotoxicity (MTT assay) Cell survival was assessed using the MTT assay. The 3-(4, 5-dimethylthiazol-2-yl)-2, 5-diphenyltetrazolium bromide dye reduction assay was performed to determine the cytotoxic effect of the AgNPs at various concentrations. The assay depends on the reduction of MTT by mitochondrial dehydrogenase, an enzyme present in the mitochondria of viable cells, to a blue formazan product. The resulting formazan was dissolved, and absorbance of the solution was read at 595 nm, according to Sriram et al. (2010). Data was analyzed using 990win6 software for DV990BV4 microplate reader, GIO DE VITA, Roma, Italy. Concentrations of AgNPs showing 50 % reduction in cell viability (i.e., IC_{50} values) was calculated.

In vivo toxicological studies A 30-day toxicity study of AgNPs was conducted in female mice, studying the survival and decrease in body weights. Twenty-four female mice were divided into four groups of six animals each. Three groups were given AgNPs of 0.1, 1.0, and 10$\mu g kg^{-1}$by i.p., once daily for 30 days. One group was served as control and was given sterile physiological saline.

Tumor models The antitumor efficacy of AgNPs in vivo was assessed by using Ehrlich ascites tumor model in mice obtained from the National Cancer Institute-Egypt, in ascetic form and was maintained by serial transplantation. Solid tumor was produced by subcutaneous implantation of Ehrlich tumor cells ($2x10^6$ viable tumor cells) into the right thigh of the lower limb of mice between the thighs subcutaneously. Before inoculation, EAC cells collected from peritoneal cavity were purified from adherent cells, and viable cells were counted by Trypan Blue exclusion test.

Animal and experimental design and tumor transplantation Mature female Swiss albino mice weighing 20±5 g were housed in the animal house of NCRRT at 22 °C±2 and fed on standard diet. Animals were quarantined for 3 weeks on a 12/12-h light/dark cycle.

Mice were divided into seven groups, (n=8). Animals were treated as: group 1 (control), received 0.1 ml of sterile saline injected i.p. Group 2 (AgNPs); animals were injected i.p. with 0.1 ml (10 μg/Kg body weight) of prepared AgNPs day after day for 15 days. Group 3 (tumor); animals were injected once with $2x10^6$ cells of Ehrlich ascites cells subcutaneously at the thighs. Group 4 (radiation); animals were exposed to fractionated dose of gamma radiation 2 Gy at a time (total dose of 6 Gy). Group 5 (tumor+AgNPs); animals bearing tumor were injected i.p. with AgNPs as group 2, day after day for 15 days. Group 6 (tumor + radiation); animals bearing tumor were exposed to gamma radiation as group 4. Group 7 (tumor + AgNPs + radiation); Animals bearing tumor were injected i.p. with AgNPs as group 2 and exposed to gamma radiation as group 4.

Mice were sacrificed, and blood was collected from the heart in heparenized tubes, tumor tissue was dissected.

Radiation process Mice irradiation was performed through the Canadian gamma cell-40 (^{137}Cs) at the National Center for Radiation Research and Technology (NCRRT-Cairo,

Egypt). The dose rate was 0.5 Gy/min. Mice whole body was exposed to a total dose of 6 Gy gamma rays as a fractionated dose with 2 Gy at a time.

Biochemical assays Weighted part of Ehrlich ascites solid tumor was homogenized in phosphate buffer saline (10 % w/v) and used for various biochemical analyses. Superoxide dismutase (SOD) and catalase (CAT) activities were determined according to Minami and Yoshikawa (1979); Aebi (1984), respectively. Reduced glutathione was determined according to Beutler et al., (1963). Malondialdehyde level was assessed as an indication to lipid peroxidation by the use of thiobarbituric acid, according to the method described by Yoshioka et al. (1979). Nitric oxide was determined according to the method of Miranda et al. (2001).

Evaluation of apoptosis and cell cycle analysis by flow cytometry Flow cytometric analysis was performed for cell cycle analysis and evaluation of apoptosis. Small intestine ileums were cut into small pieces and fixed in 70 % ethanol in phosphate buffer saline for 1 h on ice, incubated with 50 μg/ml RNase A at 37 °C overnight, stained with 50 μg/ml propidium iodide, and subjected to flow cytometric analysis using FACSCalibur. Cells were then analyzed by flow cytometry using a Becton Dickinson® FACStar Plus flow cytometer. Apoptotic cells were identified as a sub-G1 hypodiploid population (Dean and Jett 1974).

Caspase-3 assay Flow cytometric analysis for caspase-3 evaluation was performed using FITC Rabbit Anti-Active Caspase-3 of BD Pharmingen™ (Dai and Krantz 1999).

Histology Tumor tissues were stored in 10 % formalin and embedded with paraffin in wax blocks. Thin section of tumor tissue were cut using microtone and stained with hematoxylin and eosin dye solutions, examined under a light microscope.

Statistical analysis Results were expressed as mean ± Standard deviation (n=8). Statistical comparisons were performed by analysis of variance test to determine the level of significance (p<0.05). These analysis were performed using statistical package for the social science version 19 (SPSS Inc., Chicago, IL, USA) software.

3 Results

3.1 Characterization of AgNPs

Size distribution of AgNPs in the aqueous solution was evaluated by TEM images. The size distributions of AgNPs were obtained by measuring nanoparticle diameter in the images (Fig. 1). The nanoparticles shape observed by TEM were almost of spherical shape and particle sizes ranging from 8–20 nm, with a relatively narrow particle size distribution. The zeta potential of the nanoparticles was around −7.23 mV. UV–Vis spectroscopy showed a strong broad peak, located at about 430 nm for AgNPs.

Cytotoxicity of AgNPs on MCF-7 breast cancer cell line via MTT assay showed that AgNPs were able to reduce viability of the MCF-7 cells in a dose-dependent manner. AgNPs IC_{50} on MCF-7 was found to be 50 μg, which decreased the viability of MCF-7 cell to 50 % of the initial count. Further experiments were carried out to show the effect of AgNPs against solid tumor in vivo.

Mice injected with AgNPs were observed daily during the experimental period without exhibiting any abnormalities or any symptoms of toxicity such as fatigue, loss of appetite, change in fur color, or weight loss.

In order to investigate AgNPs and or irradiation on the antioxidant state, SOD, CAT, and glutathione (GSH) were evaluated. Table 1 revealed that AgNPs showed mild oxidative stress activity, while irradiation caused a depression in antioxidant state observed in the measured antioxidant parameters SOD, CAT activities, and GSH level compared to the control. Combined treatment of AgNPs with gamma irradiation showed significant depressed levels of SOD and CAT activities and GSH level compared to the control.

Silver nanoparticles, also gamma radiation, significantly increased the level of measured oxidative stress parameters of nitric oxide (NO) and lipid peroxidation (malondialdehyde, MDA) results represented in (Table 2).

Cell cycle checkpoint arrest of different treatments showed differences detected by flow cytometry analysis (Table 3). AgNPs and gamma irradiation increased apoptotic cell count compared to the control or (Eh) tumor group. On the other hand, cell cycle checkpoint was arrested at Go/G_1 with AgNPs treatment; while irradiation caused cell cycle arrest at Go/G_1 and G_2/M, while combined treatment of AgNPs with gamma radiation revealed 98 % apoptotic cells with disappear of S and G_2/M phases.

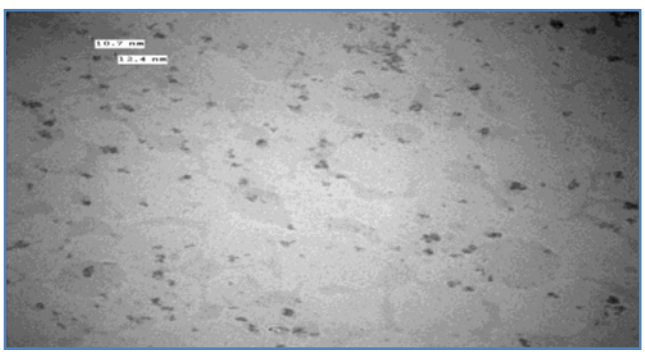

Fig. 1 TEM image of AgNPs showing a nanoparticles of spherical shape with diameter range between 8 and 20 nm

Table 1 Effect of silver nanoparticles and/or gamma radiation on SOD, CAT activities, and GSH level

Animal groups	SOD (μg/g protein)	CAT (μg/g protein)	GSH (μg/g protein)
Control	4.2±0.6	3.5±0.2	52.9±3.8
AgNPs	4.1±0.4[b]	3.1±0.1[ab]	54.8±2.5[b]
Rad	2.4±0.4[ab]	2.4±0.1[a]	44.7±2.6[ab]
Eh	3.0±0.4[a]	2.3±0.3[a]	35.3±2.9[a]
Eh + AgNPs	3.0±0.2[a]	2.4±0.2[a]	37.5±3.6[a]
Eh + Rad	2.4±0.5[ab]	1.9±0.1[ab]	40.7±2.1[ab]
Eh + Rad + AgNPs	2.7±0.3[a]	2.1±0.3[a]	34.0±3.4[ab]

[a] Significant compared to control group

[b] Significant compared to tumor bearing group

Silver nanoparticles induce apoptosis via caspase-dependent pathway. It was explored that the possible molecular mechanisms of triggering the apoptosis was identified through the activation of the caspase cascades.

Determination of apoptosis in Ehrlich ascites carcinoma tumor cells was performed using flow cytometry. Percentage of apoptotic cells counted showed that AgNPs and radiation exposure effectively induced cell apoptosis. Most of tumor cell undergo apoptosis after treatment, with AgNPs accompanied with gamma radiation, Figs. 2 and 3.

Subcutaneous implantation of Ehrlich tumor cells resulted in the development of Ehrlich solid tumor showing sheets of small and higher chromatophilic tumor cells of variable shapes, representing cell proliferation surrounding areas of necrosis and differentiated cells (Fig. 4) This picture was significantly improved in mice, given AgNPs or AgNPs with radiation as evidenced by increasing degrees of necrosis progressively increasing apoptosis.

Table 2 Effect of silver nanoparticles and/ or gamma irradiation on lipid peroxidation(MDA) and nitric oxide(NO)

Animal groups	NO (μM/g protein)	MDA (μM/g protein)
Control	4.1±0.2	9.0±0.4
AgNPs	5.3±0.5[a]	10.2±0.8[a]
Rad	6.0±0.5[a]	9.7±0.4
Eh	5.1±0.3[a]	9.8±0.3
Eh + AgNPs	5.1±0.3[a]	11.5±1.0[ab]
Eh + Rad	5.7±0.6[ab]	10.2±0.8[a]
Eh + Rad + AgNPs	6.6±0.8[ab]	12.0±0.8[ab]

[a] Significant compared to control group

[b] Significant compared to tumor bearing group

Table 3 Cell cycle analysis of Ehrlich ascites tumor cells in response to AgNPs treatment and gamma irradiation

Animal groups	subG$_1$ (%)	Go/G$_1$ (%)	S (%)	G$_2$/M (%)
Control	9.9±3.2	7.57±0.9	3.4±0.4	1.2±0.04
AgNPs	68.3±5.2[ab]	12.5±1.0[ab]	4.3±0.3[ab]	1.3±0.05[ab]
Rad	52.0±3.2[ab]	12.0±1.6[ab]	4.0±0.3[ab]	2.8±0.05[a]
Eh	32.3±3.4[a]	19.5±2.9[a]	5.8±0.3[a]	3.1±0.04
Eh + AgNPs	81.8±2.8[ab]	10.3±0.9[ab]	2.1±0.3[ab]	1.5±0.03[ab]
Eh + Rad	71.7±2.6[ab]	13.97±1.0[ab]	4.8±0.6[ab]	2.9±0.05[a]
Eh + Rad + AgNPs	98.1±3.0[ab]	0.38±0.1[ab]	0.0±0.0[ab]	0.00±0.0[ab]

[a] Significant compared to control group

[b] Significant compared to tumor bearing group

4 Discussion

There is an increasing interest towards the exploitation of silver nanoparticles technology in the development of bioactive biomaterials because of its distinctive properties, such as good conductivity, chemical stability, catalytic, antibacterial activity, antifungal, antiviral, and antiinflammatory (Mukherjee et al. 2001; Sondi and Branka 2004; Chen and Schluesener 2008). Silver is a common substance used by the Mexican people for disinfecting foods and water for their consumption. It was documented that silver intake as colloidal silver provided in the water at 10- and 50-fold higher concentrations than recommended by the manufacturer during 1 year did not show any alterations in the evaluated parameters (fertility, birth, and tumors development) (Franco-Molina et al. 2010).

Silver is one of the most effective antibiotic substances known and has been used to treat human ailments for over100 years due to its natural antibacterial and nontoxic properties. The free silver ion has two distinctive antimicrobial mechanisms. The first involves denaturation of the disulfide bonds of bacterial proteins, which form the essential elements of bacterial structure and become disjointed to

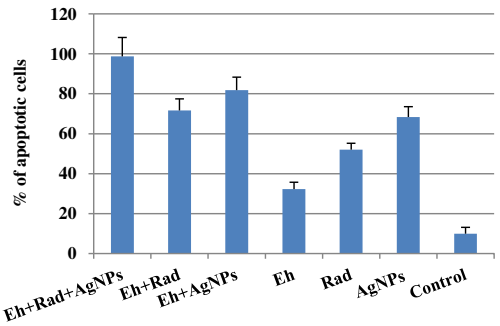

Fig. 2 Percentage count of apoptotic cells of Ehrlich ascites tumor cells in response to AgNPs and gamma irradiation

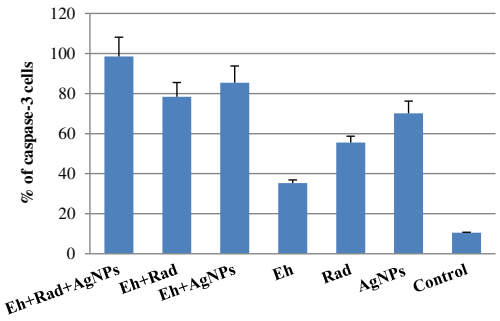

Fig. 3 Percentage count of Caspase-3 activated cells of Ehrlich ascites tumor cells in response to AgNPs and gamma irradiation

the catalytic effect of silver ion. The second involves oxidation, where ionized silver helps to generate reactive oxygen in the air, which in turn attach around the cell, preventing it from reproduction, and cause cell death (Thurman and Gebra 1989; Gurunathan et al. 2009).

In this study, AgNPs synthesized were of average size 8–20 nm and zeta potential of −7.23 mV by the biological method using a technique involving electrostatic interaction between positively charged amino group in the extract and negatively charged Ag ions, producing negatively charged AgNPs. This approach is simple, does not use toxic chemicals, and is amenable for large-scale production.

Particle size and zeta potential are important properties, which may influence the biological activity of nanoparticles and has been suggested as a key factor through the interaction with charged surfaces. Nanoparticles with different particle size or zeta potential may have different mechanisms of inhibition (Bihari et al. 2008).

In this study, AgNPs in vitro conditions exerted dose-dependent cytotoxic effect on MCF-7. Tumor cells assessed by MTT assay and LC_{50} value were found to be 3.5 ng. The cytotoxic effect of AgNPs on cell viability is the result of active physicochemical interaction of silver atoms with the functional groups of intracellular proteins, as well as with the nitrogen bases and phosphate groups in DNA (Sriram et al. 2010).

Ehrlich carcinoma is an undifferentiated carcinoma that is originally hyperdiploid and has high transplantable capability, no regression, rapid proliferation, short life span, 100 % malignancy, and also does not have tumor-specific transplantation antigen. Ehrlich carcinoma has a resemblance with human tumors, which are the most sensitive to chemotherapy, due to the fact that it is undifferentiated and has a rapid growth rate (Ozaslan et al. 2011). Generally, implantation of Ehrlich tumor cells is followed by morphological and metabolic changes such as structural deterioration, decreased number of mitochondria, decreased DNA and RNA synthesis, loss of intracellular purine and pyrimidine nucleotides, nucleosides and bases, a decline of ATP concentration and turnover, decreased protein synthesis, decreased glutathione concentration and increased triglycerides, cholesterol esters, and free fatty acids (Segura et al. 2001).

In the present study, subcutaneous implantation of Ehrlich tumor cells into the right thigh of the lower limb of mice resulted in a significant decrease in tissue CAT, SOD enzyme activities, and GSH, with a significant increase in MDA and NO levels compared to the normal control group. These results were in agreement with Badr El-Din (2004); Zahran et al. (2008).

Results in the present study of mice bearing tumor that received AgNPs or gamma radiation or combined treatment of AgNPs and gamma radiation showed a marked decrease in SOD and CAT activities and GSH level accompanied with increase in NO and MDA levels. This could be a result of enzyme degradation due to extreme oxidative damage caused by radiation or Ag (Borek 2004) or to mitochondrial damage, which decrease mitochondrial Mn–SOD activity, leading to decrease in total SOD (Ueda et al. 1996) and depletion of GSH content, which is utilized during detoxification of the free radicals generated by radiation or AgNPs and enhances lipid peroxidation (Jagetia and Reddy 2005; Wambi et al. 2008). Due to the inhibition of SOD,

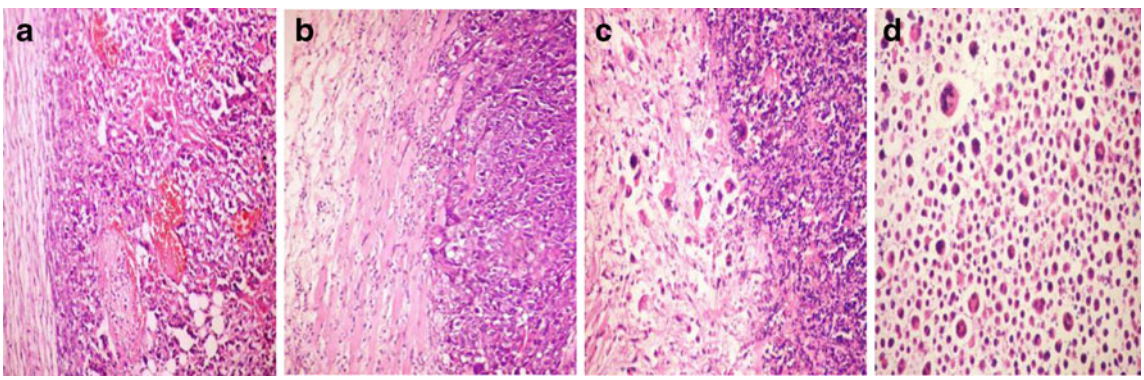

Fig. 4 Photomicrograph of Ehrlich ascites tumor sections from mice. **a** Control section showing sheets of malignant cells with lot of dilated congested blood vessels (H&E ×400). **b** and **c** Section in the Ehrlich ascites tumor that received AgNPs showing malignant cells with necrotic and apoptotic cells and reduced blood vessels (H&E ×200 and 400, respectively). **d** Section from mice that received AgNPs and gamma radiation showing most cells in necrosis and apoptosis stage also fragmented cell constituents (H&E ×400)

superoxide anion radicals may be combined with nitric oxide to form peroxynitrite anion, which initiates lipid peroxidation. The decrease in the levels of antioxidant enzymes are in close relationship with the induction of lipid peroxidation. Silver nanoparticles was reported to cause a marked increase in NO and MDA levels (Park et al. 2010).

The antitumor activity of nanoparticles and silver is suggested to induce their toxicity through oxidative stress and inflammation by generating reactive oxygen species (ROS) involved in a variety of different cellular processes ranging from apoptosis and necrosis to cell proliferation and carcinogenesis (Sarkar et al. 1998). Intracellular reduced GSH scavenge ROS generated in cells to be oxidized to glutathione disulphide (GSSG). AgNO3 penetrated the cell membrane and reacted with GSH, depleted its contents mostly due to oxidation of reduced GSH to GSSG 2 GSH-GSSG+2H+or likely that Ag^{2+} after penetration formed a silver–glutathione complex(Khan et al. 2011).

The production of high levels of ROS molecules and hydrogen peroxide (H_2O_2) lead to cell death (Kim et al. 2007). The H_2O_2 causes cancer cells to undergo apoptosis and necrosis. In contrast, normal cells are considerably less vulnerable to H_2O_2. The reason for the increased sensitivity of tumor cells to H_2O_2 is not clear but may be due to lower antioxidant defenses. It is well-known that H_2O_2 exerts dose-dependent effects on cell function, from growth stimulation at very low concentrations to growth arrest, apoptosis, and eventually necrosis as H_2O_2 concentrations increase (Mazurek et al. 1992). The increased sensitivity of tumor cells to killing by H_2O_2 provides the specificity and "therapeutic window" for the antitumor therapy (Frei and Lawson 2008).

It is commonly accepted that SOD protects against free radical injury by converting O^{2-} radical to H_2O_2, which can be removed by CAT and prevent the formation of $OH^{\bullet}$ radical. Due to the inhibition of SOD, superoxide anion radicals may be combined with nitric oxide to form peroxynitrite anion, which initiates lipid peroxidation. The decrease in the levels of antioxidant enzymes are in close relationship with the induction of lipid peroxidation. These results are in accordance with many studies, which reported that the inhibition of antioxidant systems in blood and tissues of mice and rats was accompanied by an increase in lipid peroxide products after irradiation exposure (Zhao et al. 2007). Also, Borek (2004) mentioned that when the oxidative damage is extreme as a result of irradiation, ROS scavenging enzymes such as SOD and CAT are degraded. Ueda et al. (1996) postulated that the decrease in SOD level could be due to mitochondria damage and decrease of mitochondria Mn–SOD activity, which leads to a decrease in total SOD in different tissues of rats exposed to radiation.

Results of this study clarified that AgNPs induced cell cycle arrest at G1, while a combined treatment of AgNPs with irradiation induced marked cell cycle arrest at S, G_2/M phases. AgNPs significantly increase ROS and DNA breakage with high levels of apoptosis and necrosis. Silver nanoparticles are capable of adsorbing cytosolic proteins on their surface that may influence the function of intracellular factors. Moreover, downregulation of genes necessary for cell cycle progression (cyclin B and cyclin E) and DNA damage response/repair, modulate gene expression and protein functions, leading to defective DNA repair, and cell proliferation arrest (Oberdörster et al. 2005; Gopinath et al. 2008; Rani et al. 2012).

In the present study, histopathological findings accompanied with cell cycle analysis results showed that AgNPs showed antiangiogensis effect by decreasing blood vessels with increase in apoptotic cells. Gamma radiation showed synergistic effect with AgNOs revealing marked increase in apoptotic cells. AgNPs may induce apoptosis via oxidative stress (Arora et al. 2008; Gopinath et al. 2008), since many studies have implicated intracellular ROS in the signal transduction pathways leading to apoptosis (Ott et al. 2007; Ueda et al. 2002). Antiangiogenic effect of AgNPs could be due to its direct inhibitory effect on epithelial cells viability during vascular endothelial growth factor induced angiogenesis in endothelial cells. Thereby, inhibiting the development of angiogenic disorders (Gurunathan et al. 2009). AgNPs may block the proliferation and migration of BREC, which are essential for generation of new blood vessels from existing vessels or de novo angiogenesis in endothelial cells (Kalishwaralal et al. 2009).

In order to clarify the mechanism by which AgNPs exert cytotoxic effect in tumor cells, a caspase-3 analysis by flow cytometry was performed. In the present study, induction of apoptosis by AgNPs with or without gamma radiation in Ehrlich ascites tumor cells was mediated with significant induction of caspase-3, which mediates apoptosis. Detection of caspases provides early biochemical detection of apoptosis (Ha et al. 1998).

Thus, the result of this study demonstrated that aqueous dispersions of silver nanoparticles exhibit antitumor properties in vitro and in vivo. In conclusion, AgNPs might be a potential alternative agent for cancer treatment and a sensitizing agent for radiotherapy. However, more studies are needed to elucidate the mechanism of AgNPs action for the treatment of cancer and other illness, with lower cost and effectiveness.

References

Aebi H (1984) Catalase in vitro. Methods Enzymol 105:12

Arora S, Jain J, Rajwade JM, Paknikar KM (2008) Cellular responses induced by silver nanoparticles: in vitro studies. Toxicol Lett 179:93–100

Badr El-Din NK (2004) Protective role of sanumgerman against cirradiation-induced oxidative stress in Ehrlich carcinoma bearing mice. Nutr Res 24:271–291

Bihari P, Vippola M, Schultes S, Praetner M, Khandoga A, Reichel C et al (2008) Optimized dispersion of nanoparticles for biological in vitro and in vivo studies. Part Fiber Toxicol 5:14

Beutler E, Duron O, Kelly BM (1963) Improved method of the determination of blood glutathione. J Lab & Clin Med 61(5):882

Borek C (2004) Dietary antioxidants and human cancer. Inter Cancer Ther 3:333–341

Chen X, Schluesener HJ (2008) Nanosilver: a nanoproduct in medical application. Toxicol Lett 176(1):1–12

Dai C, Krantz SB (1999) Interferon gamma induces upregulation and activation of caspases 1, 3, and 8 to produce apoptosis in human erythroid progenitor cells. Blood 93(10):3309–3316

Dean PN, Jett JH (1974) Brief note: mathematical analysis of DNA distributions derived from flow microfluorometry. J Cell Biol 60(2):523

Franco-Molina AM, Mendoza-Gamboa E, Sierra-Rivera CA, Gómez-Flores RA, Zapata-Benavides P, Castillo-Tello P, Alcocer-González JM, Miranda-Hernández DF, Tamez-Guerra DF, Cristina Rodríguez-Padill C (2010) Antitumor activity of colloidal silver on MCF-7 human breast cancer cells. J Exp Clin Cancer Res 29:148–155

Frei B, Lawson S (2008) Vitamin C and cancer revisited. Proc Natl Acad Sci USA 105:11037–11038

Gopinath P, Sonit KG, Arun C, Siddhartha SG (2008) Implications of silver nanoparticle induced cell apoptosis for in vitro gene therapy Nanotechnology 19(7):5104

Gurunathan S, Kalishwaralal K, Vaidyanathan R et al (2009) Purification and characterization of silver nanoparticles using *Escherichia coli*. Colloid Surf B Biointerfaces 74:328–335

Ha HC, Woster PM, Casero RA (1998) Unsymmetrically substituted polyamine analog induces caspase-independent programmed cell death in bcl-2-oveproducting cells. Cancer Res 58:2711–2714

Jagetia GC, Reddy TK (2005) Modulation of radiation-induced alteration in the antioxidant status of mice by naringin. Life Sci 77:780–794

Kalishwaralal K, Banumathi E, Pandian SRK, Deepak V, Muniyandi J, Eom SH (2009) Silver nanoparticles inhibit VEGF induced cell proliferation and migration in bovine retinal endothelial cells. Colloid Surf B 73:51–57

Khan H, Khan MF, Asim-ur-Rehman, Jan SU, Ullah N (2011) The protective role of glutathione in silver induced toxicity in blood components. Pak J Pharm Sci 24(2):123–128

Kim DW, Hong GH, Lee HH, Choi SH, Chun BG, Won CK, Hwang IK, Won MH (2007) Effect of colloidal silver against the cytotoxicity of hydrogen peroxide and naphthazarin on primary cultured cortical astrocytes. Neuroscience 117(3):387–400

Law N, Ansari S, Livens FR, Renshaw JC, Lloyd JR (2008) The formation of nanoscale elemental silver particles via enzymatic reduction by Geobacter sulfurreducens. Appl Environ Microbiol 74:7090–7093

Mazurek S, Zander U, Eigenbrodt E (1992) In vitro effect of extracellular AMP on MCF-7 breast cancer cells: inhibition of glycolysis and cell proliferation. Cell Physiol 153(3):539–549

Minami M, Yoshikawa MA (1979) A simplified assay method of superoxide dismutase activity for clinical use. Clin Chim Acta 92:337

Miranda KM, Espey MG, Wink DA (2001) A rapid simple spectrophotometric method for simultaneous detection of nitrate and nitrite. Nitric Oxide 5(1):62–71

Mukherjee P, Ahmad A, Mandal D, Senapati S, Sainkar Sudhakar R, Khan MI, Renu P, Ajaykumar PV, Alam M, Kumar R, Sastry M (2001) Fungus-mediated synthesis of silver nanoparticles and their immobilization in the mycelial matrix: a novel biological approach to nanoparticle synthesis. Nano Lett 1:515–519

Oberdörster G, Maynard A, Donaldson K, Castranova V, Fitzpatrick J, Ausman K, Carter J, Karn B, Kreyling W, Lai D, Olin S, Monteiro-Riviere N, Warheit D, Yang H (2005) A report from the ILSI Research Foundation/Risk Science Institute Nanomaterial Toxicity Screening Working Group, Principles for characterizing the potential human health effects from exposure to nanomaterials: elements of a screening strategy, Particle and Fibre Toxicology, 2:8

Ott M, GogvadzeV, Orrenius S, Zhivotovsky B (2007) Mitochondria, oxidative stress and cell death. Apoptosis 12:913–922

Ozaslan M, Karagoz ID, Kilic IH, Guldur ME (2011) Ehrlich ascites carcinoma. Afr J Biotechnol 10(13):2375–2378

Park H. S., Jang S., Cha H. R., Park J. W., Shin J. Y., Kim S. Y., Koo J. S. and Kim J. O. (2010) Silver nanoparticles induce apoptosis by regulation of cyclic AMP response element-binding protein in lung cancer cells. Cancer Prevention Research. 3(12) Supplement 2

Philip D (2009) Biosynthesis of Au, Ag, and Au-Ag nanoparticles using edible mushroom extract. Spectrochim Acta A 73:374–381

Rajesh WR, Niranjan SK, Jaya RL, Vijay DM, Sahebrao BK (2010) "Extracellular synthesis of silver nanoparticles using dried leaves of pongamia pinnata (L) pierre", Nano-Micro Lett 2(2):106–111

Rani PVA, Hande MP, Valiyaveettil S (2009) Antiproliferative activity of silver nanoparticles. BMC Cell Biol 10:65

Rani PVA, Sethu S, Lim KH, Balaji G, Valiyaveettil S, Hande MP (2012) Differential regulation of intracellular factors mediating cell cycle, DNA repair, and inflammation following exposure to silver nanoparticles in human cells. Genome Integr 3:2

Sarkar S, Yadav P, Bhatnagar D (1998) Effect of cadmium on glutathione metabolism and glucose 6-phosphate dehydrogenase in rat tissues: role of vitamin E and selenium. Trace Elem Electrolytes 15:101–105

Segura JA, Ruiz-Bellido MA, Arenas M, Lobo C, Marquez J, Alonso FJ (2001) Ehrlich ascites tumor cells expressing antisense glutaminase RNA lose their capacity to evade the mouse immune system. Int J Cancer 91:379–384

Sondi I, Branka S (2004) Silver nanoparticles as antimicrobial agent: a case study on *E. coli* as a model for Gram-negative bacteria. J Colloid and Interfac Sci 275:177–182

Sriram MI, Kanth SBM, Kalishwaralal K, Gurunathan S (2010) Antitumor activity of silver nanoparticles in Dalton's lymphoma ascites tumor model. Int J Nanomed 5:753–762

Thurman RB, Gerba CHP (1989) The molecular mechanisms of copper and silver ion disinfection of bacteria and virus. Crit Rev Environ Control 18:295–315

Tian J, Wong KY, Ho C, Lok C, Yu W, Che C, Chiu J, Tam PKH (2007) Topical delivery of silver nanoparticles promotes wound healing. Chem Med Chem 2(1):129–136

Ueda S, Masutani H, Nakamura H, Tanaka T, Ueno M, Yodoi J (2002) Redox control of cell death. Antioxid Redox Signal 4(3):405–414

Ueda TY, Toyoshima T, Moritani K, Ri N, Otsuki T, Kushihashi H, Yasuhara T, Hishida (1996) Protective effect of dipyridamole against lethality and LPx in liver and spleen of the ddY mouse after whole-body irradiation. Int J Radiol Biol 69:199–20

Wambi C, Sanzari J, Wan XS, Nuth M, Davis J, Ko Y-H, Sayers CM, Baran M, Ware JH, Kennedy AR (2008) Dietary antioxidants protect hematopoietic cells and improve animal survival after total-body irradiation. Radiol Res 169:384–396

Yoshioka T, Kawada K, Shimada T, Mori M (1979) Lipid peroxidation in maternal and cord blood and protective mechanism against activated oxygen toxicity in the blood. Am J Obstet Gynecol 135:372

Zahran MA, Salem TA, Samaka RM, Agwa HS, Awad AR (2008) Design, synthesis, and antitumor evaluation of novel thalidomide dithiocarbamate and dithioate analogs against Ehrlich ascites carcinoma-induced solid tumor in Swiss albino mice. Bioorg Med Chem 16(22):9708–9718

Zhao W, Diz DI, Robbins ME (2007) Oxidative damage pathways in relation to normal tissue injury. Br J Radiol 80:S23–S31